Proceedings of the Fourth IASTED International Conference
POWER AND ENERGY SYSTEMS (PES 2008)
April 2-4, 2008 Langkawi, Malaysia
ISBN Hardcopy: 978-0-88986-731-4 / CD: 978-0-88986-732-1

AN IMPROVED ALGORITHM FOR MPPT OF PHOTOVOLTAIC SYSTEM BY ZERO –VOLTAGE SWITCHING TECHNIQUE

Chamnan. Ratsame[2], Tanes. Tanitteeapan[1] , Sirichai. Thepa[2] , Narong. Mungkung[1] , Itsda Boonyaroonate[3]

[1] Department of Electrical Technology Education
Faculty of Industrial Education and Technology
[2]Division of Energy Technology.
School of Energy Environment and Materials.
[3] Department of Electrical Engineering
Faculty of Engineering
King Mongkut' s University of Technology Thonburi ,Bangmod, Thong-kru , Bangkok 10140, Thailand
Email addresses:
Chamnan.rat @kmutt.ac.th ,tanes_kmutt@yahoo.com , sirichai.the(at)@kmutt.ac.th

ABSTRACT
This paper deals with the design and experimental implementation of a maximum power point tracking (MPPT) for photovoltaic system , The MPP-tracker proposed in this paper is a study the quasi – square ware resonant switch (QSW) DC-DC buck converter the choice for many high efficiency converter that have many advantage when compared with conventional zero voltage switching quasi resonant switches and zero voltage transition(ZVT) converter. which is a this type DC-DC buck converter operating in continuous and discontinuous conduction mode(CCM/DCM) to depend on change of load. The converter is able to draw maximum power from the PV system for a given irradiation level by adjusting the duty cycle of converter. Analytical models are built for the PV system and converter on the basis of the data sheet of manufacturer and the principle of energy conservation. The control technique, implement with a single-chip microcontroller ADMC331, is based on the Hill-climbing / P&O method. From the result obtained it can be concluded that , the MPPT can increase the overall efficiency of the system 87 % for conventional converter. While, the overall efficiency of the converter efficiency when the zero voltage switching by this current technique is used increases 94 % under different atmospheric condition. The accuracy of the proposed scheme is confirmed by experimental.

KEY WORDS
Photovoltaic, MPPT , PI controller, Hill – climbing / Perturbation and Observation Algorithm, QSW- Buck converter

1. Introduction

Photovoltaic(PV) generation assumes increased importance as a renewable source due to advantages such as the absence of fuel cost, little maintenance and no noise and wear due to absence of moving parts. However, Two important factors limit the implementation of photovoltaic systems i.e. high cost and low efficiency in energy conversion. In photovoltaic systems, the PV panel represents 57% of the total cost of the system, and the battery storage system corresponds to 30% of the cost. Other system components such as inverters and maximum power point tracker contribute only with 7% (Hua and Lin, 2003). Due to the high cost of solar cells. Therefore, controlling maximum power point tracking (MPPT) for the photovoltaic system is essential in a PV system. The amount of power generated by a PV system depends on the operating voltage of the array. While a maximum power point (MPP) of PV system varies with solar insulation and temperature. Its V-I and V-P characteristic curves specify a unique operating point at which maximum possible power is delivered. At the MPP, the PV operates at its highest efficiency. Therefore, many methods have been developed to determine MPPT. Three popular tracking methods based on power feedback are widely adopted in PV power systems. They are the perturbation and observation method(P&O) [2], the incremental conductance method (IncCond) [3] and the hill climbing method (HC). Both P&O and InCond are based on the same technology by regulating the PV array's voltage to follow an optimal set point, which represents the voltage of maximum power operating point . This point is continuously tracked and updated to satisfy a simple mathematical equation: dP/dV = 0, where P represents the PV module's output power and V represents the PV voltage., the maximum power points can always be tracked if we keep dP/dV equal to zero., MPP-trackers have been widely implemented with several techniques and power conditioners. In the work developed by Maheshappa et al., the PV array voltage is compared with a constant reference voltage, which corresponds to the PV voltage at the maximum power point, under specific atmospheric conditions, as MPP will depend on the chosen reference. In the work proposed by Medeiros and Antunes, the neural network requires a new training at each change of the system size. The incremental conductance method (Solodovnik et al., 2004) leads to good accuracy in tracking the MPP even under rapidly changing weather, but a digital signal processor (DSP) is necessary in the implementation.

Soft switching techniques have been widely used in reducing the switching losses and EMI noises of switching mode power converter. Soft switching techniques, especially zero voltage switching (ZVS) have become more and more popular in the power supplies industries. The Quasi resonant buck converter employing the ZVS technique was first introduced by Tabis et al.[7] This converter provides ZVS condition for the main switch without increasing voltage stress of the active switches. However, it has s disadvantage such as the as the auxiliary switching circuit is turned off with hard - switching which deteriorates the overall efficiency , increase EMI noises and power loss , switches has high cost.[8],[9],[10] Within this text, this work presents the design and experimental implementation of a real time maximum power point tracker for photovoltaic systems. The MPP-tracker proposed in the paper is a study the quasi – square ware resonant switch (QSW) DC-DC buck converter the choice for many high efficiency converter that have many advantage when compared with conventional zero voltage switching quasi resonant switchs and zero voltage transition(ZVT) converter, To operating in continuous conduction mode(CCM).The Hill - climbing /P&O algorithm searches the maximum power pint according to irradiation. The algorithm is implemented using microcontroller ADMC 331,whose output signal set the duty cycle of pulse width modulation (PWM) buck converter.

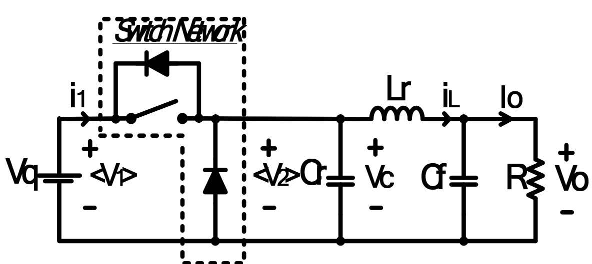

Figure 1. Proposed QSW buck converter

2. Mathematical Model

2.1 Basis Principal of the PV-Cell

Fig.2. shows the typical equivalent circuit of PV-cell. The typical I-V output characteristics of PV-cell are represented as following (1).

$$I = I_{SC} - I_o \left\{ \exp\left[\frac{q\left(V + R_S I\right)}{nKT_K} \right] - 1 \right\} - \frac{V + R_S I}{R_{sh}} \qquad (1)$$

where V and I represent the output voltage and current of the PV respectively: R_s and R_{sh} are the series and shut resistance of cell ; q is the electronic charge ; I_{sc} is the light generated current ; I_o is the reverse saturation current ; n is a dimension factor ; k is the Boltzman Constance and T_k is the temperature in k^o . Equation (1) was used in computer simulations to obtain characteristics of solar cell.

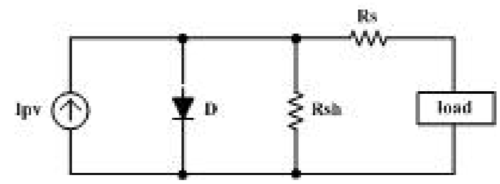

Figure 2. The equivalent model of photovoltaic

Figure. 3(a) shows the typical I-V and P-V output characteristic curve of PV- module. Fig. 2(b) show the typical P-V output characteristic curves of P-V module in the case that the irradiance is varied.

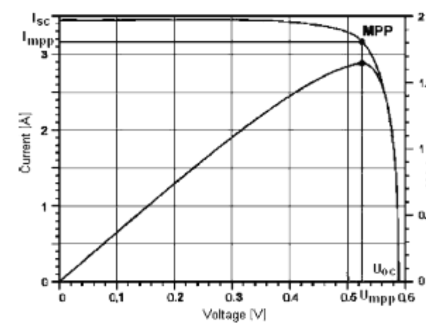

(a) Type characteristic curve

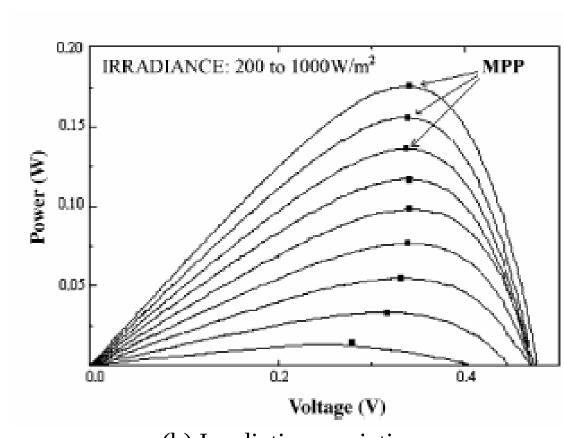

(b) Irradiation variations

Figure 3. The output characteristic curves of PV-cell

From Fig.3(b). we know that the output characteristic of PV-module are nonlinear and each curve only has one maximum power point (MPP) . Additionally , the output current of PV- module is mainly affected by irradiation variation , whereas the output voltage of PV-module is mainly affected by temperature variation . therefore, to efficiently use PV-module, in case the atmospheric condition are varied, the maximum power point tracking of PV-module should be implemented.

2.2 Equivalent quasi- square ware buck converter

In steady – state operation, a conventional buck converter, as show in Fig.4 can be treated as a constant current source , I ,supplying power to a constant voltage load ,V_o , by means of duty cycle control of the switch (s.w). When switch (s.w) is replaced by the voltage mode resonant switch of L_r and C_r , a voltage – mode quasi resonant buck converter , as shown in Fig 4.(b). Sine the circuit's behavior is largely determined by the values of L_r and C_r , the following parameters are defined as

1) characteristic impedance $R_o = \omega_o L$
2) resonant angular frequency $\omega_o = 1/\sqrt{L_r C_r}$
3) resonant frequency $f_o = \left(\omega/2\right)\pi$
4) normalized load resistance $r = \sqrt{\dfrac{L_r}{C_r}}$

In steady- state operation , a complete switch cycle can be divided into five stages starting form the moment switch turns off, before switch is turned off, it curries the input current ,I. Diode D_2 is turned on and no current is flowing into the voltage load , V_o. At time T_0, switch turns on , input current I_1 is diverted into capacitor C_r . The following description summarized the circuit operation each of the five stages.

Stage 1 [T_0 - T_1]: Linear charging to t = T_0, the main switch is turn-on , and main diode D_2 is turn-off. The voltage and current expressions in the state plane trajectory of this stage are given by

$$V_C(t) = \langle V_1 \rangle = V_g \tag{2}$$

$$\frac{di_L(t)}{dt} = \frac{V_g - V_0}{L} = \langle V_1 \rangle \frac{1-\mu}{L} \tag{3}$$

At time t = T_1 ; $\omega_O t = \alpha$

$$i_L\left(\frac{\alpha}{\omega_o}\right) = I_{L1} = \langle V \rangle \frac{1-\mu}{L}\frac{\alpha}{\omega_O} \tag{4}$$

Normalized : current inductance , voltage capacitor the switching interval are defined in terms per unit of this mode are given by :

$$J_{L1} = (1-\mu)\alpha \quad ; Define \frac{J_{L1}}{1-\mu} = \alpha \tag{5}$$

$$m_C = \frac{V_C}{V_{base}} = 1 \tag{6}$$

Stage 2.[T_1 – T_2]: Resonant stage, the resonant inductance current I_{Lr} reaches I_{in}, L_r and C_r begins to resonant charging of inductor and discharging of capacitance. The initial conditions of this stage are $J_L = J_{L1}$; $m_C = 1$, $J_L = J_{L2}$; $m_C = 0$ respectively.

$$r_1^2 = (1-\mu)^2 + J_{L1}^2 \tag{7}$$

$$r_1^2 = (1-\mu)^2 + J_{L2}^2 \tag{8}$$

Finally ,

$$J_{L2} = \sqrt{1 - 2\mu + J_{L1}^2} \tag{9}$$

Therefore, At interval length of resonant stage is given by

$$\beta = \tan^{-1}\left(\frac{1-\mu}{J_{L1}}\right) + \tan^{-1}\left(\frac{\mu}{J_{L2}}\right) \tag{10}$$

Stage 3 [T_2 – T_3]: Linear Discharge when V_{c1} reaches zero the main diode D_1 is turn-off witch ZVS at t = T_3. The voltage and current expressions in the state plane trajectory of this stage are given by

$$V_C(t) = 0 \tag{11}$$

$$\frac{di_L(t)}{dt} = \frac{-V_0}{L} = \langle V_1 \rangle \frac{\mu}{L} \tag{12}$$

At end of interval length ; $\omega_O t = \delta$

$$-I_{L2} = \left(\frac{-\mu\langle V_1 \rangle}{L}\right)\left(\frac{\delta}{\omega_0}\right) \tag{13}$$

Normalized : current inductance , voltage capacitor the switching interval are defined in terms per unit of this mode are given by :

$$J_{L2} = \mu\delta \quad ; Define \frac{J_{L2}}{\mu} = \delta \tag{14}$$

$$m_C = 0 \tag{15}$$

Stage 4 [T_3 – T_4]: At T_3 , the resonant inductor and resonant capacitor begins to resonant and conducts current at $\mu > 0.5$. At this instant, main switch can be turn-on due to internal diode reversed bias, The resonant capacitor voltage is equal to V_g at t = T_4 , The voltage and current expression are given by:

$$r_2^2 = \mu^2 = J_{L3}^2 + (1-\mu)^2 \tag{16}$$

$$J_{L3}^2 = \sqrt{2\mu - 1} \tag{17}$$

$$\xi = \pi - \tan^{-1}\left(\frac{J_{L3}}{1-\mu}\right) \tag{18}$$

Stage 5 [T_4 – T_5]: At T_4 when the increasing voltage of resonant capacitor across is greater then V_g , the diode D_1 is turn-on under ZVS. The operation of the circuit at this stage is identical to the normal turn-on operation of a PMW buck converter to begin a new switching cycle.

$$V_C(t) = \langle V_1 \rangle \tag{19}$$

$$\frac{di_L}{dt} = \frac{\langle V_1 \rangle - \mu \langle V1 \rangle}{L} \tag{20}$$

Therefore, At end of interval length $\omega_o t = \varsigma$

$$I_{L3} = \frac{\langle V_1 \rangle - \mu \langle V_1 \rangle \varsigma}{L\omega_O} \tag{21}$$

Normalize of this stage equation

$$I_{L3} = (1 - \mu)\varsigma \tag{22}$$

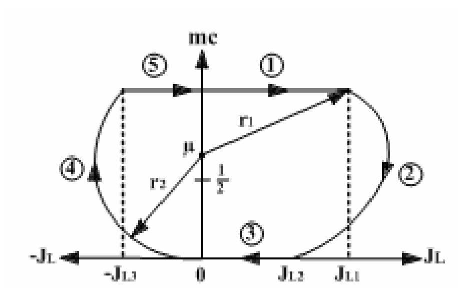

Figure 4. Normalized state plane trajectory

The proposed buck converter has five operation stage. The ideal normalized resonant capacitor voltage and inductor current ware plotted to the state plane trajectory shown in Fig. 4 and Fig .5 respectively.

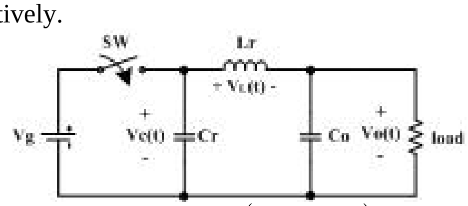

(a) Stage 1. $(T_0 \le t \le T_1)$

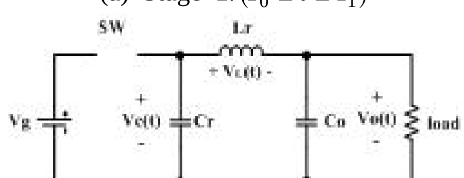

(b) Stage 2. $(T_1 \le t \le T_2)$

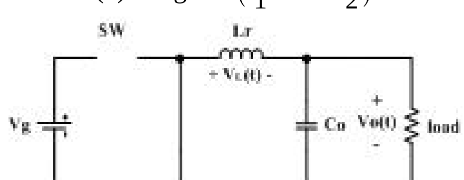

(c) Stage 3. $(T_2 \le t \le T_3)$

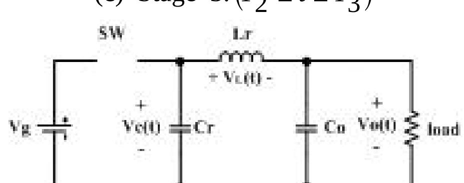

(d) Stage 4. $(T_3 \le t \le T_4)$

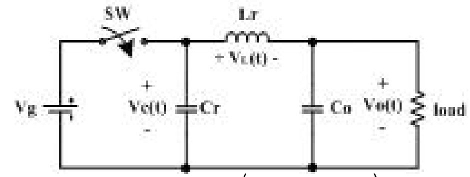

(e) Stage 5. $(T_4 \le t \le T_5)$

Figure 5. Equivalent circuit of each operation stage

To determination of switching frequency plays a most important role in the design of the power converter. There are many factors influence its proper selection. However, the determination of switching frequency is still a compromise between theoretical analysis and practical implementation. In this paper, the analysis and design of a quasi – square ware resonant switch buck converter is selected 100 KHz switching frequency . In the design procedure of resonant capacitor and resonant inductance can be expressed as

$$C_r = \frac{1}{\omega_O} \tag{23}$$

$$L_r = \frac{R_O}{\omega_O} \tag{24}$$

where parameter, ω_O is angle frequency., the switching frequency period is the one interval length period to be expressed as following.

$$\omega_O T_S = \alpha + \beta + \xi + \varsigma = \frac{2\pi}{F} \tag{25}$$

Therefore, equation of duty cycle can be as expressed

$$d = \frac{\theta}{\omega_O T_S} = \frac{\theta F}{2\pi} \tag{26}$$

2.3 Characterization of PI control

PI controllers are in most cases analyzed and tuned in the continuous time domain. The corresponding transfer function is given as following

$$U(s) = \left(K_P + \frac{K_I}{s} \right) \times I(s) \tag{27}$$

where I and U denote the input error signal and controller ' s output, s is the Laplace variable and K_p and K_I are the two parameter of the PI controller associated with the proportional (P) and integral (I) part. Equation (27), the transition from the continuous to the discrete time domain entail that the integral operation has to be by Zero order hold (ZOH). Such as can now be shown in the following.

$$U(z) = \frac{K_P z + K_P(\omega_{PI}.T_{sample} - 1)}{z - 1}.I(z) \tag{28}$$

Therefore, it is to make reverse phase.

$$U_{K+1} = K_P \times I_{K+1} + P_P(\omega_{PI}.T_{sample} - 1)I_K + U_K$$

$$U_{K+1} = A_1.I_{K+1} + A_0.I_K + U_K \tag{29}$$

Equation (29), the signal is sampled at the instant k and held constant until the next sampling instant k+1.

2.4 Maximum Power Point Tacking

Maximum power point tracking means that PV module is always supposed to operate at maximum output voltage rating. A MPPT is a DC/DC converter that sets the PV module to operate at MPP independently of the load. The diagram of the MPP-tracking proposed in this work is shown in Fig.3., Using a power MOSFET IRFZ24N is PWM controller, operating with switching frequency equal to 100 KHz. Adjusting the duty cycle of switching. The MPP- tracking control circuit is implemented with microcontroller ADMC 331. The schematic of the MPP- tracking proposed in this work is shown in Fig. 6

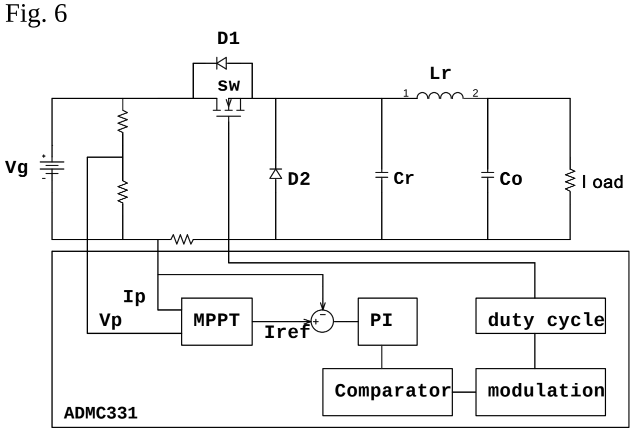

Figure 6. The diagram of the implemented system

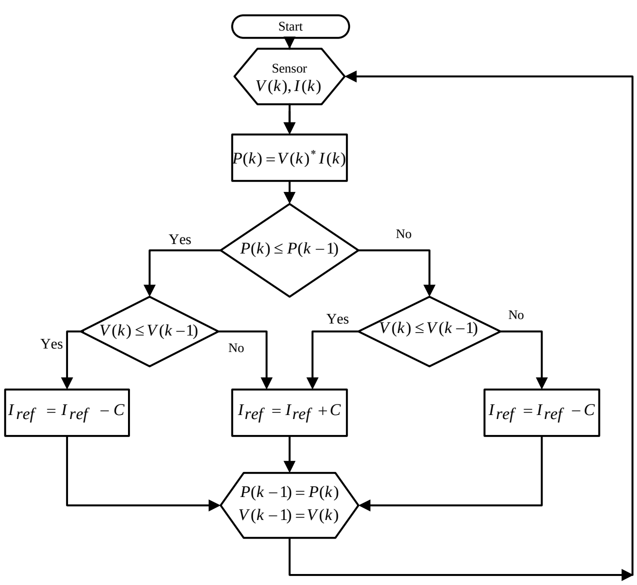

Figure 7. Algorithm MPPT flowchart control

A simple algorithm based on Hill- climbing and Perturbation and observation (P&O) method has been developed for real time track., and then it can fail under rapidly changing atmospheric condition. In the method described in [2], the power converter is controlled using the PV module output power. Figure.7 is based on the calculation of the PV output power and of the power change by sampling voltage and current values. The power change is detected by comparing the present and previous voltage levels, in order to calculate a reference voltage which is used to produce the PWM control signal. The DC/DC converter is driven by a DSP-based controller for fast-response and the overall system stability is improved by including a PI controller which is also used to match the array and reference voltage levels. However, the DSP-based control unit increases the implementation cost of the system.

The specifications and components of QSW-buck converter are given in Table 1 and Table 2 respectively.

Table 1
Specifications of the QSW – buck converter

Output Power, P_O	60 W
Switching frequency, f_s	100 KHz
Output voltage ripple, Δv_o	0.05
Estimated efficiency, η	$\ge 92\,\%$

Table 2
Component used in prototype

Component	Value / Model
Switches	IRFZ24N
Diode	MUR 1520
Resonant Inductance (L_r)	16 μH
Resonant capacitor (C_r)	53.912 nF
Output capacitor (C_o)	100 μF
Controller single chip	ADMC331

3. Experimental results

The proposed photovoltaic system was implemented using a DSP-based control with microcontroller ADMC 331. The system consists of a nonlinear current source as the power source, the PV-module electrical characteristic ware Voc = 21.6 V, Isc = 4.72 A, Imax = 3.1 A , V_{max} = 17.3 V; there are the manufacturer rated values under standard operating condition., a resistor set as the load is 60 watt load. Such as design of resonant inductor and resonant capacitor of quasi square ware resonant switching (QSW) buck converter., that the inductor value is calculated as 16 μH. The output capacitor and resonant capacitor value are calculated as 100 μF,53.93 uF respectively. Taking into account that the ripple of the PV output current must be less than 20%. The switching frequency is 100 KHz. In order To improve the efficiency of the DC-DC buck converter is using zero voltage switching by quasi square ware resonant technique (QSW), That circuit transfers to the load the energy that would be dissipated during turning on and turning off. From a laboratory arrangement has been implemented in order to verify the performance of the maximum power point tracker proposed in this work, and also the performance of zero voltage switching (ZVS) of QSW buck converter, For simulation results shown in Figs. 8-11, one can see that switching losses during turning on and turning off are drastically reduced when the soft switching cell is used. The simulation was implemented under real time changing irradiation condition. For testing the MPP tracking, the performance of the PV system is studied for a clear sunny day with various radiation level on 15th June 2007 at King Mongkuk's University of Technology Thonburi (KMUTT) in Bangkok. All measurements ware recorded by a data logger every 5 second from 10 A.M to 2.30 P.M time.

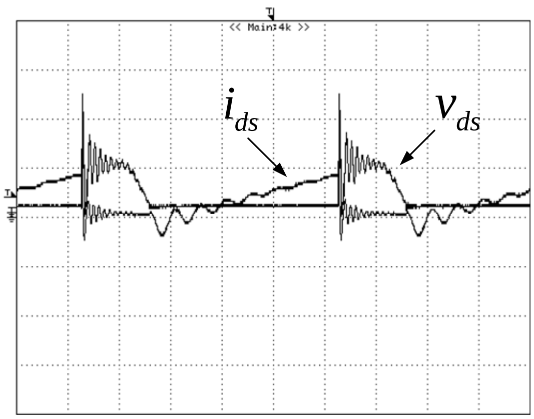

Vertical CH1 : 20V/div, CH2 : 5A/div
Horizontal 2uS/div

Figure 8. Voltage and Current ware forms of $S1$ for the proposed ZVS buck converter

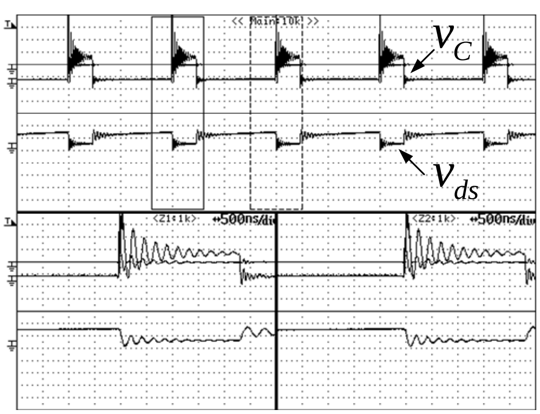

Vertical CH1 : 10V/div, CH2 : 5A/div
Horizontal 5uS/div

Figure 8. Voltage and Current ware forms of $S1$ for soft -switching buck converter

A lot of measurements have been made different sky condition. Figure.12. show of the experiment results gathered using the algorithm. Which refers to different irradiation., As can be observed, the system is stable and operates successfully even in cases of changing atmospheric condition., PV system output power(W) and input power (W) has been plotted, in Fig.13, versus time to show how well the device tracked. Figure.14 has been plotted to show efficiency versus time. Thus , experiment result confirm the method proposed.

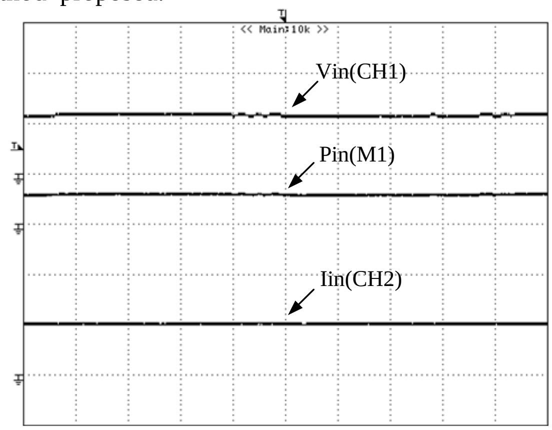

Vertical CH1:10V/div, CH2:5A/div, M1:50W/div
Horizontal 10us/div

Figure 9. Voltage, Current and input power ware forms of QSW - buck converter For soft switching buck converter

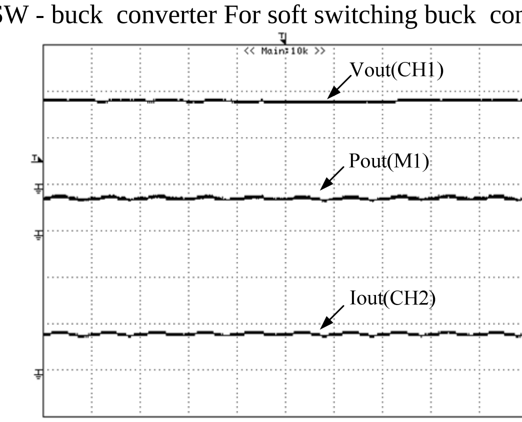

Vertical CH1:10V/div, CH2:5A/div, M1:50W/div
Horizontal 10us/div

Figure 10. Voltage, Current and output power waveforms of QSW - buck converter

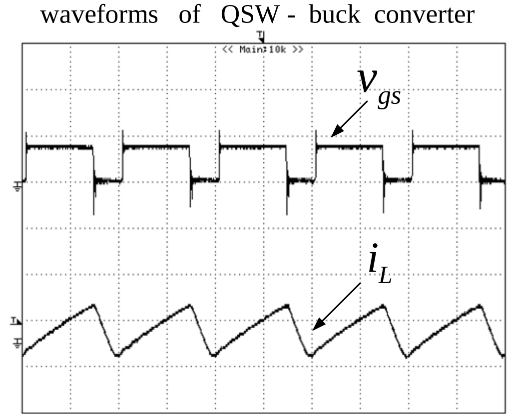

Vertical CH1 : 20V/div, CH2 : 5A/div
Horizontal 5uS/div

Figure 11. Inductor current and duty cycle waveforms of QSW - buck converter

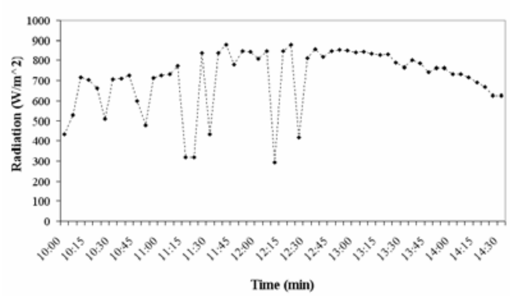

Figure 12. Irradiance (W/m^2) vs. time waveforms on 15th June 2007

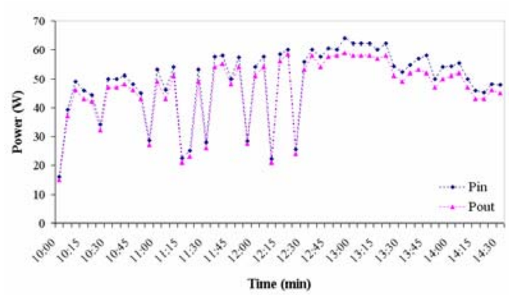

Figure 13. Output power (W) and input power (W) vs. Time For a MPPT programmed with the Algorithm on 15th June 2007

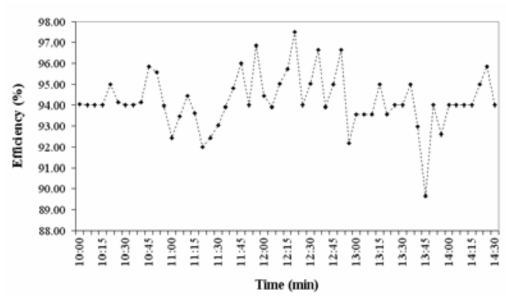

Figure 14. Efficiency vs. time for a MPPT programmed with the algorithm on 15th June 2007

4. Conclusion

The purpose of maximum power tracking is to transfer the maximum available power to the resistance load form the PV system. The MPP-Tracking is a boost converter , The use of microcontroller allows simple modification of the system, controlled by a single chip microcontroller that employs the Hill- climbing / P&O algorithm. Experiment results describe the performance of the designed MPP-tracking . The MPP-tracking increased about 24 % the energy transfer from the PV system to load and the overall efficiency of the MPP-tracking system about 87 %. Fig.14 shows result representing collected data of the converter efficiency when the zero voltage switching by this current technique is used increases 94 % due to the additional energy that is transferred to the load. The results show that proposed MPP- tracking algorithm has successful tracked the MPP in changing illumination condition.

Acknowledgements

This work was in part supported by Power Electronic and Motor Drive Laboratory (PEMD) Department of Electrical Engineering and by Department of Electrical Technology Education KMUTT.

References

[1] Hua and Lin, 2003 C. Hua and J. Lin, An on-line MPPT algorithm for rapidly changing illuminations of solar arrays, *Journal of Renewable Energy* 28 (2003), pp. 1129–1142.

[2] C. Hua, J. Lin, and C. Shen, "Implementation of a DSP- Controlled photovoltaic system with *peak* power tracking", *IEEE Trans Induslrial Elecfroni*~v~o.l. 45, pp. 99 -107, Feb. 1998

[3] K.H Hussein, I.Muta, T. Hoshino, and M. Osaka, Maximum photovoltaic power tracking: an algorithm for rapidly changing atmospheric conditions", in *IEE Proc. Gemmion. Trammission and Disfribulion.* vol. 142**,** p p . 5 9 4 , Jan. 1995

[4] Medeiros and Antunes, 1998 Medeiros, A., Antunes, F., 1998. A neural network-based real time maximum power tracking controller for grid connected PV system. IEEE-IECON'98, Aachen, Germany, pp. 554–558.

[5] Maheshappa et al., 1998 H.D. Maheshappa, J. Nagaraju and M.V. Krishna Murthy, An improved maximum power point tracker using a step-up converter with current locked loop,*Renewable* Energy 13 (1998) (2), pp. 195–201.

[6] Solodovnik et al., 2004 E.V. Solodovnik, L. Shengyi and R.A. Dougal, Power controller design for maximum power tracking in solar installations, *IEEE Transactions on Power Electronics.* (2004), pp. 1295–1304.

[7] Tabisz, W.A.,Gradzki, P>M. and Lee, F.C.Y, 1980. " Zero - Voltage – Switched Quasi- Resonant Buck and Flyback Converter- Experimental Results at 10 MHz," IEEE Trans on Power Electronics, Vol. 4, pp. 194 – 204.

[8] Maksimovic, D., 1993, " Desing of The Zero – Voltage - Switching Quasi – Square – Ware Resonant Switch," Power Electronics Specialists Conference, PESC' 93 Record , 24th Annual IEEE, 20-24 June 1993 , pp. 323 - 329